


ORIGINAL ARTICLE

Characterizing the metabolic role of STAT3 in canine osteosarcoma

Heather L. Gardner¹  | Joelle M. Fenger² | Ryan D. Roberts³ | Cheryl A. London¹

¹Cummings School of Veterinary Medicine, Tufts University, North Grafton, Massachusetts, USA

²College of Veterinary Medicine, The Ohio State University, Columbus, Ohio, USA

³Research Institute at Nationwide Children's Hospital, Columbus, Ohio, USA

Correspondence

Heather L. Gardner, 200 Westboro Rd., North Grafton, MA, USA.

Email: heather.gardner@tufts.edu

Present address

Joelle M. Fenger, Ethos Veterinary Health and Ethos Discovery (501c3), Woburn, Massachusetts, USA

Funding information

Animal Cancer Foundation; Morris Animal Foundation; NCI NIH, Grant/Award Numbers: P01CA165995, K08CA201638; NIH Office of the Director, Grant/Award Numbers: K01OD019923, K01OD028268; Sarcoma Foundation of America

Abstract

Signal transducer and activator of transcription 3 (STAT3) dysregulation has been characterized in canine OS, with previous data suggesting that constitutive STAT3 activation contributes to survival and proliferation in OS cell lines in vitro. Recently, the contribution of STAT3 to tumour metabolism has been described across several tumour histologies, and understanding the metabolic implications of STAT3 loss may elucidate novel therapeutic approaches with synergistic activity. The objective of this work was to characterize metabolic benchmarks associated with STAT3 loss in canine OS. STAT3 expression and activation was evaluated using western blotting in canine OS cell lines OSCA8 and Abrams. STAT3 was deleted from these OS cell lines using CRISPR-Cas9, and the effects on proliferation, invasion and metabolism (respirometry, intracellular lactate) were determined. Loss of STAT3 was associated with decreased basal and compensatory glycolysis in canine OS cell lines, without modulation of cellular proliferation. Loss of STAT3 also resulted in diminished invasive capacity in vitro. Interestingly, the absence of STAT3 did not impact sensitivity to doxorubicin in vitro. Our data demonstrate that loss of STAT3 modulates features of aerobic glycolysis in canine OS impacting capacities for cellular invasions, suggesting a role for this transcription factor in metastasis.

KEYWORDS

canine, comparative oncology, metabolism, osteosarcoma, STAT3

1 | INTRODUCTION

Despite three decades of effort, canine osteosarcoma (OS) remains a therapeutic challenge, with no improvements in patient outcome observed for over three decades. Macroscopic metastases are extremely refractory to treatment, including chemotherapy and kinase inhibitors (i.e., toceranib) necessitating the identification of novel targets for therapeutic intervention.^{1,2} Consequently, increased emphasis has been placed on targeting recently defined aberrant signalling pathways in canine OS, such as those involving MAPK and PI3K/mTOR, among others.³⁻⁹

Signal transducer and activator of transcription 3 (STAT3) is a transcription factor that mediates a number of critical biologic

processes, including cellular differentiation and proliferation, cell cycle progression, inflammation and apoptosis by transmitting cytokine signals through gp130.^{10,11} These activities are traditionally associated with STAT3 phosphorylation on conserved tyrosine 705 (Y705) residues, with subsequent homodimerization and nuclear translocation.¹² More recently, studies are increasingly ascribing non-canonical functions to STAT3, including cellular metabolism mediated by mitochondrial STAT3, STAT3 acetylation resulting in methylation of tumour suppressor genes such as *CDKN2A*, and dimerization and transcriptional activation of unphosphorylated STAT3.¹²⁻¹⁷ In human cancers, STAT3 dysregulation is typically a due to upstream drivers, including IL-6 family cytokines, G-protein coupled receptors and non-receptor

This is an open access article under the terms of the [Creative Commons Attribution-NonCommercial-NoDerivs](https://creativecommons.org/licenses/by-nc-nd/4.0/) License, which permits use and distribution in any medium, provided the original work is properly cited, the use is non-commercial and no modifications or adaptations are made.

© 2022 The Authors. *Veterinary and Comparative Oncology* published by John Wiley & Sons Ltd.

tyrosine kinases (e.g., SRC, ABL).^{10,16} Constitutive phosphorylation of STAT3 has also been previously described in canine OS, with both SRC and IL-6 receptor/gp130 identified as upstream drivers of activation. In canine OS cell lines, pSTAT3 promoted survival and proliferation in vitro, which was inhibited by STAT3-targeting small molecule inhibitors or STAT3 knockdown using siRNA.^{7,18–21} DeltaNp63, a splice variant of p63 that does not contain the N-terminal transactivation domain, is overexpressed in both canine and human OS.²² In human and canine OS, DeltaNp63 is associated with increased IL-6 (human) and IL-8 (canine and human) secretion, resulting in STAT3 phosphorylation and VEGF secretion, supporting a role in tumour angiogenesis.^{22,23} Additionally, deltaNp63 expression has been shown to be higher in OS pulmonary metastases, and has been associated with enhanced invasive capacity of canine OS cell lines and pulmonary metastasis in vivo.^{22–24} Furthermore, IL-6 and IL-8 have been shown to act as drivers of pulmonary tumour cell seeding in canine OS, but has no effect on primary tumour growth, together supporting a role for canonical STAT3 activation by cytokines in OS metastasis.²⁴

One increasingly recognized non-canonical function of STAT3 is tumour metabolism. A metabolic switch in the mitochondria leading to increased electron transport chain (ETC) activity and mitochondrial superoxide production has been associated with a pro-metastatic phenotype in human and murine cancer cell lines.²⁵ Interestingly, this effect involves the tyrosine kinase Src, an upstream driver of STAT3 which was previously noted to be constitutively activated in canine OS lines.^{18,25} Consequently, the purpose of this work was to characterize the metabolic implications of STAT3 loss in canine OS cell lines as a foundation for future investigation of rationale therapeutic combinatorial approaches.

2 | MATERIALS AND METHODS

2.1 | Cell lines and primary tumour samples

The canine OS cell lines: OSCA-2 and OSCA-8 were obtained from Dr. Jaime Modiano (University of Minnesota, Minneapolis, MN, USA). The Abrams cell line was provided by Dr. Douglas Thamm (Colorado State University, Fort Collins, CO, USA). The canine D17 cell line was purchased from ATCC (Cat #: CCL-183).

The Abrams cell line was cultured in DMEM media with 10% foetal bovine serum (FBS) and 1% penicillin/streptomycin, 1% HEPES (4-[2-dihydroxyethyl]-1-piperazineethanesulphonic acid), 1% NEAA (non-essential amino acids). The OSCA-2, OSCA-8 and D17 cell lines were cultured in RPMI 1640 with 10% FBS and 1% penicillin/streptomycin, 1% HEPES, 1% sodium pyruvate and 1% NEAA. All cells were cultured at 37°C in 5% CO₂. All media and media supplements were purchased from Gibco (Thermo Fisher Scientific).

2.2 | Cell line validation statement

Cell lines were routinely tested for mycoplasma via standard PCR prior to initiating experimental protocols. All canine cell lines were

confirmed to be of canine origin via species-specific multiplex PCR, as previously described.^{26,27} STR profiling of canine cell lines was performed using commercially available loci (StockMarks Applied Biosystems). One-tenth of the resultant PCR reaction was used for fragment analysis. Loci are reported in Table S1, and compared to available published loci.²⁶

2.3 | Western blot

Protein was extracted from cell lines using fresh complete lysis buffer (20 mM Tris-HCl pH 8.0, 137 mM NaCl, 10% glycerol, 1% IPEGAL CA-630, 10 mM ethylenediaminetetra-acetic acid (EDTA), 1 mg/ml aprotinin, 1 mg/ml leupeptin, 1 mg/ml pepstatin A, 1 mM phenylmethylsulphonyl fluoride, 1 mM sodium orthovanadate, and 10 mM sodium fluoride (all from Sigma), quantified using the Bradford assay, and transferred to a PVDF membrane after separation via SDS-PAGE, as previously described.²⁸ Membranes were blocked in 5% bovine serum albumin dissolved in tris-buffered saline with 0.1% Tween20 (TBST) or 3% nonfat dry milk in TBST, for phospho-proteins and non-phospho proteins, respectively. Membranes were incubated with primary antibodies as indicated in Table S2 at 4°C overnight; HRP-linked secondary antibodies were used at a dilution of 1:20000. SuperSignal West Dura Extended Duration Substrate (ThermoFisher Scientific) was incubated on the membranes 3 min prior; membranes were sealed in clear plastic sheet protectors prior to film exposure.

2.4 | CRISPR-Cas9 cell lines

Forward and reverse oligos (Table S3) designed to target STAT3 or a non-targeting scramble control were annealed using 1M Tris (pH 8.0), 0.5 M EDTA and 2.5M NaCl, and ligated into the lentiCRISPRv2 plasmid, a gift from Feng Zhang (Addgene plasmid #52961; <http://n2t.net/addgene:52961>; RRID:Addgene_52961).²⁹ Ligation was performed using Quick Ligase (New England Biolabs [NEB] M2200S), and *E. coli* (NEB Stable Competent *E. coli* C3040H) were transformed per manufacturer recommendations. Guide insertion was confirmed using sanger sequencing. Lentivirus was isolated from 293T cells transfected with a non-targeting scramble control or targeting lentiCRISPRv2 plasmid using polyethylenamine (PEI; Polysciences: #23966-1). Target OS cells were transduced with lentivirus and polybrene (Millipore: #TR-1003-G), per manufacturer recommendations. After puromycin selection, monoclonal lines were isolated, and the resulting STAT3 expression was confirmed via western blotting.

2.5 | Intracellular lactate

Intracellular lactate was determined enzymatically using a Lactate-Glo Assay (Promega: #J5022) per manufacturer recommendations. Twenty-thousand cells were seeded in opaque 96-well plates and incubated 24 h at 37°C in 5% CO₂. Cells were washed with PBS and

lysed according to published recommendations.³⁰ Luminescence was determined after a 1-h incubation, and total intracellular lactate concentration was determined by a standard curve.

2.6 | Seahorse assays

OS cell lines were plated at a density of 20 000 cells/well in 96-well plates (Agilent) and incubated 24 h at 37°C in 5% CO₂. Oxygen consumption rate (OCR) and extracellular acidification rate (ECAR) were measured using a Seahorse XFe96 Extracellular Flux analyzer (Agilent). Prior to initiating the assay, standard cell culture media was replaced with Agilent Seahorse XF Base Medium (Agilent: #103335) or Agilent Seahorse XF RPMI Medium (Agilent: # 103336) supplemented with 1 mM Na pyruvate, 2 mM glutamine, 10 mM glucose and HEPES (5 mM DMEM, 1 mM RPMI), all from Gibco. All OS cell lines were subjected to the Agilent Seahorse XF Cell Mito Stress Test (Agilent: #103015-100) or the Agilent Seahorse XF Glycolytic Rate Assay (Agilent), per manufacturer recommendations. All compounds used in these assays were obtained from Sigma Aldrich as follows: 2-deoxy-D-glucose (2-DG) (Sigma: #D6134), Oligomycin (Sigma: #O4876), Rotenone (Sigma: #R8875), Antimycin A (Sigma: #A8674) and carbonyl cyanide-4 (trifluoromethoxy) phenylhydrazone (FCCP) (Sigma: #C2920). Briefly, for Cell Mito Stress Tests, basal respiratory measurements were initially taken prior to injection of oligomycin (Complex V/ATP synthase inhibitor), resulting in decreased mitochondrial respiration linked to ATP production. FCCP is injected into the system, which uncouples respiration from the proton gradient and permits cells to reach maximal uninhibited respiratory capacity. Finally, rotenone (Complex I inhibitor) and antimycin A (Complex III inhibitor) inhibit all mitochondrial respiration and are utilized as a positive control in the system. Regarding the Glycolytic rate assay, proton efflux rate is measured as extracellular acidification and is composed of both CO₂ from mitochondrial respiration and protons from the breakdown of lactate. After measurement of extracellular acidification and oxygen consumption, rotenone and antimycin A are injected to inhibit sources of cellular acidification derived from mitochondrial respiration. Measurements taken thereafter are reflective of compensatory glycolysis. Finally, 2-DG (hexokinase inhibitor) is injected to inhibit glycolysis and is utilized as a positive control for the experiment.

OCR and ECAR readings were normalized to protein concentration (using a Bradford assay) or cell count (as estimated from a standard curve analysed using the sulphorhodamine B assay). Assays were performed with six technical replicates and repeated at least three times.

2.7 | Proliferation assays

For the sulphorhodamine B assay: OS cells were seeded in 96-well plates at a density of 2500 cells/well and incubated 24, 48, and 72 h. Cells were fixed with 10% trichloroacetic acid and stained with 0.04% sulphorhodamine B, as previously described.³¹

For the CyQUANT Cell Proliferation Assay: OS cells were seeded in 96-well plates at a density of 2500 cells/well and incubated 24 h at 37°C in 5% CO₂, prior to the addition of doxorubicin (Pfizer) (0, 0.06, 0.11, 0.23, 0.45, 0.91, 1.81, 3.344 μM), after which cells were incubated an additional 24 h. The CyQUANT Cell Proliferation Assay (Molecular Probes, Inc.) was performed as previously described.²¹ Proliferation was calculated as a fraction of the untreated control. The IC50 was calculated after plotting proliferation on a logarithmic scale.

2.8 | Transwell invasion assays

OS cell lines were plated at a density of 100 000 cells/transwell and the assay was performed as previously described.³² Briefly, cells were plated in the upper chamber in media containing 0% FBS and allowed to invade into the lower chamber containing 10% FBS over 24 or 48 h. Inserts were processed as previously described.³² Cells were plated in duplicate and experiments were repeated three times. Cells from 10 random fields were counted and averaged for each transwell assay. The mean and SE across all biologic replicates are reported.

2.9 | Statistical analyses

Invasion assays were performed in duplicate and repeated three times. Seahorse assays were performed with six technical replicates and repeated three times. All other assays were performed in triplicate and repeated three times. For analysis of SRB proliferation assays, a linear regression model was used; $p < .05$ was considered significant. A 2-way ANOVA was used to determine significance of Seahorse assay experiments, to account for multiple factors. Intracellular lactate and Matrigel invasion assays were analysed using a 1-way ANOVA. All analyses were completed using GraphPad Prism 7.0.4 (GraphPad Software). All statistical tests referenced the parental (wild-type) cell line for comparisons.

3 | RESULTS

3.1 | STAT3 is phosphorylated in a subset of canine OS cell lines

Expression of STAT3 was confirmed in canine OS cell lines using western blotting. Consistent with previous studies, canine OS lines express STAT3, and exhibit constitutive activation of STAT3, as determined by phosphorylation on the Y705 residue (Figure 1). As STAT3 has previously been evaluated in the Abrams and OSCA-8 cell lines using siRNA techniques and small molecule inhibitors, we chose these cell lines for downstream functional studies.¹⁸⁻²⁰

3.2 | Loss of STAT3 is associated with decreased basal and compensatory glycolysis in canine OS cells, but does not alter cellular proliferation

We next sought to assess the metabolic effects of STAT3 loss in canine OS lines. Two measures of metabolic capacity were utilized:

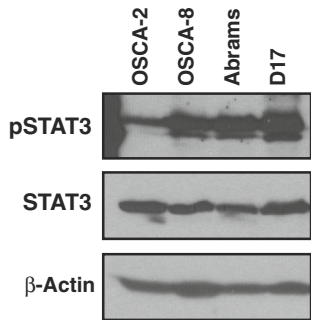


FIGURE 1 STAT3 is activated in canine OS. Western blot demonstrating expression of pSTAT3 and STAT3 in canine OS cell lines. Protein lysates are representative of one biologic replicate, and were not pooled across multiple passages.

respirometry and intracellular lactate concentration. Notably, canine OS cell lines exhibited downregulation of basal and compensatory glycolysis, without downregulation of cellular proliferation in the absence of STAT3 (Figure 2). This suggests that while the canine cell lines utilize glycolysis to meet their energetic needs, they readily use the mitochondrial electron transport chain in the absence of STAT3. Consistent alterations in basal or maximal mitochondrial respiration, ATP production and intracellular lactate were not observed in canine OS cell lines in which STAT3 was deleted (Figure 2, Figures S1 and S2). However, a trend towards an inverse correlation between baseline glycolytic and oxidative parameters was noted. For example, in cells where basal respiration was decreased, glycolysis was not significantly depressed, supporting the notion that cells utilize alternate bioenergetic pathways to meet metabolic requirements in vitro. Finally, the percent PER from glycolysis in Abrams cells was consistently higher in comparison to the OSCA-8 line, indicating variability in the relative contribution of glycolysis to extracellular acidification across OS cell lines (Figure 3).

Interestingly, we noted that with prolonged passaging, the percentage of proton efflux solely from glycolysis trended upwards in the OSCA-8 line (Figure 3A), suggesting metabolic adaptation in this cell line with prolonged passaging. In contrast, the Abrams cell

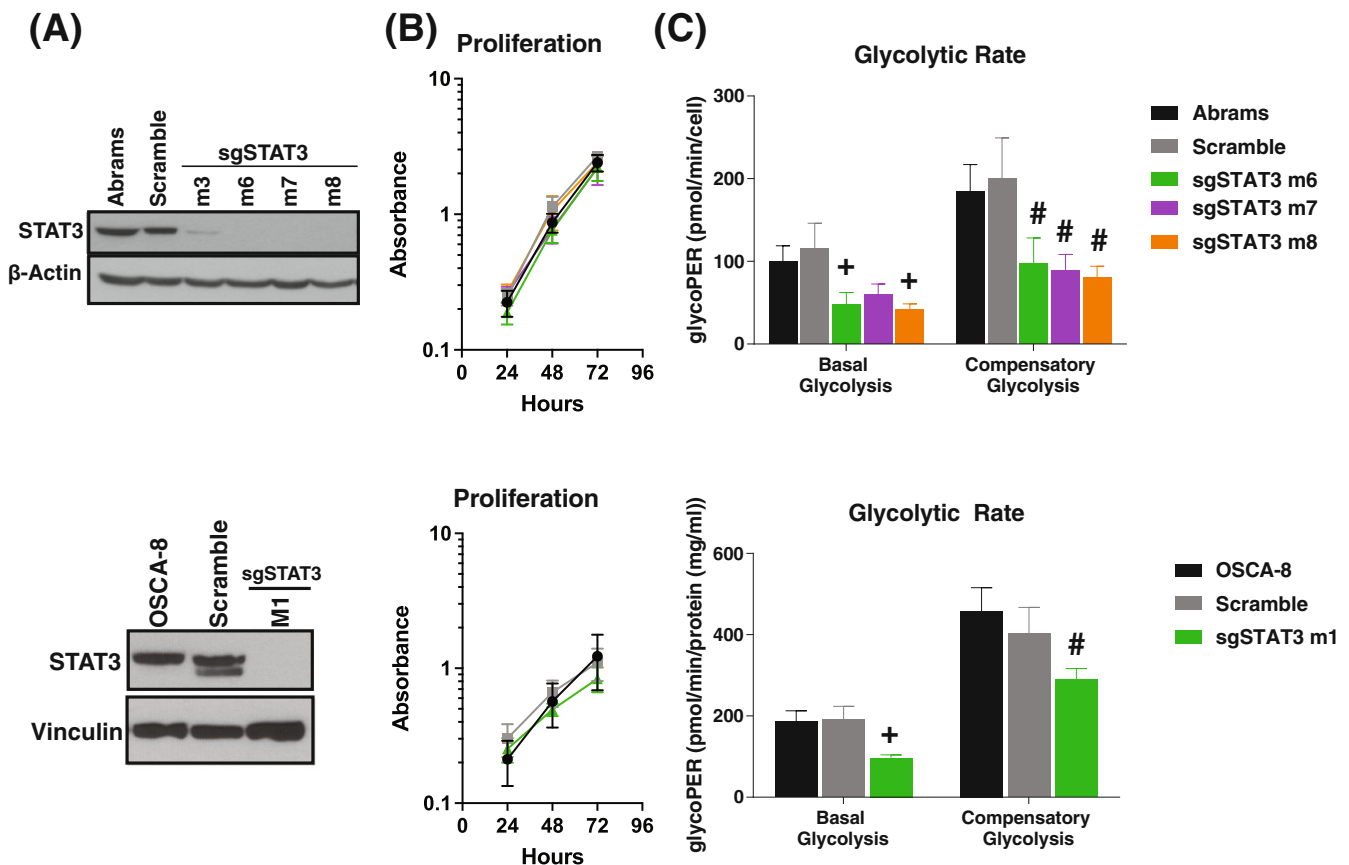


FIGURE 2 Effect of STAT3 on cellular proliferation and glycolytic rate. (A) Representative western blot confirming STAT3 deletion in canine OS cell lines. (B) Proliferation over 72 h was determined in STAT3 knockout lines using the SRB assay. Results are presented as the mean \pm SD across three biologic replicates. $p < .05$ was considered significant. (C) Basal and compensatory glycolysis were determined in STAT3 knockout cell lines using the Seahorse XFe Glycolytic Rate Assay. Results of one representative biologic replicate are shown as mean \pm SD. $p < .01$ was considered significant. M(#)=monoclonal cell line. $^+p < .01$; $^{\#}p \leq .001$

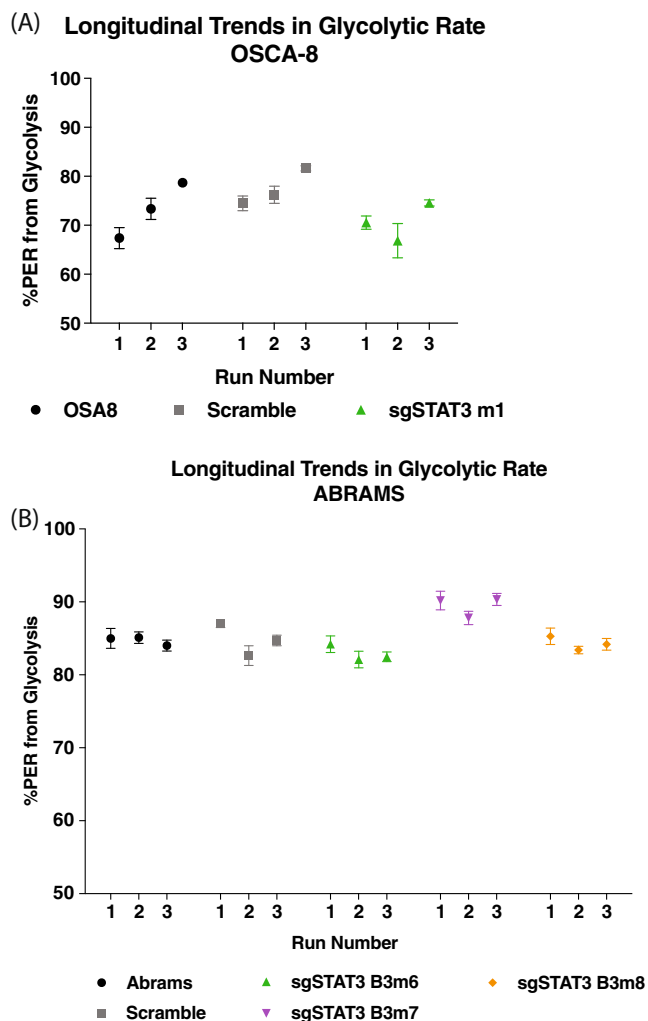


FIGURE 3 Longitudinal Trends in Glycolytic Rate. Percent proton export rate (%PER) in (A) OSCA-8 and (B) Abrams cell lines across biologic replicates using the Seahorse XFe Glycolytic Rate Assay. Error bars represent the mean \pm SD.

line remained relatively stable throughout passaging (Figure 3B), indicating that any differences in glycolytic proton efflux rate in this line over time were due to STAT3 inhibition. Together, these findings stress the importance of tracking tumour cell line adaptability following gene editing, particularly with repeated passage in vitro.

3.3 | Loss of STAT3 results in decreased invasive capacity without modulating cellular proliferation

The invasive capacity of OS cells lacking STAT3 was assessed in the Abrams and OSCA-8 cell lines using a transwell invasion assay. In both the Abrams and OSCA-8 cell lines, the invasive capacity of OS cells was reduced in the absence of STAT3, consistent with previous studies (Figure 4).^{21,23}

3.4 | Loss of STAT3 does not enhance chemosensitivity

We next explored whether STAT3 deletion sensitized cells to cytotoxic chemotherapy. Doxorubicin was of considerable interest because (1) it is a common component of frontline chemotherapy in OS and (2) is known to have effects on the mitochondria through inhibition of Complexes I and II of the electron transport chain, thereby impacting a source of NAD⁺ regeneration.^{33,34} In the Abrams OS cell line, loss of STAT3 did not alter sensitivity to doxorubicin exposure over 24 h as determined by cellular proliferation (Figure 5A). However a possible effect of the lentiCRISPR plasmid was observed in the OSCA8 line (Figure 5B) as both the scramble and STAT3 deficient clones exhibited an increased sensitivity to doxorubicin. Together these findings highlight the importance of correlating metabolic dysregulation with functional outcomes.

4 | DISCUSSION

STAT3 has been extensively studied as a potential therapeutic target in several cancers, including OS, and increasing evidence supports coordinated metabolic and nuclear transcriptional STAT3 activity across various tumour types.^{21,35,36} However, successful development of STAT3-specific inhibitors with clinical efficacy has remained a challenge.^{35,36} The purpose of this study was to characterize the effects of STAT3 loss on features of tumour cell metabolism and correlate them with the canonical transcriptional functions of STAT3 in canine OS to identify metabolic biomarkers that may influence response to STAT3 inhibition.

In the current study, we assessed the effects of STAT3 loss using CRISPR-Cas9 based knockout in OS cell lines. Consistent with previous reports, we found that cells deficient in STAT3 demonstrated impaired invasive capacity, concordant with previous studies in canine and human OS.^{21,37} While STAT3 mediated effects on tumour cell invasive capacities have been associated with direct alteration of transcriptional targets, our data support the notion that STAT3 also contributes to metabolic adaptations likely necessary to confer a survival advantage in the tumour microenvironment.³⁸ Interestingly, deletion of STAT3 using CRISPR-Cas9 did not cell proliferation, which is a departure from historical data in canine OS.¹⁸⁻²¹ This discrepancy highlights the differential effects of gene deletion, transient knockdown and target inhibition with small molecules when evaluating protein function in tumour cell lines. Prior studies in canine OS utilized STAT3 small molecule inhibitors or transient siRNA transfection.^{7,18-21} Therefore, it is possible that the previously reported impact of STAT3 on cellular proliferation and viability were due to off-target effects of small molecule inhibitors or short-term/incomplete STAT3 downregulation. Importantly, our findings are consistent with emerging data in human OS cell lines in which inhibition of STAT3 has little impact on cellular proliferation.³⁷ Future work should therefore incorporate multiple assessments of cellular proliferation after short-term and long-term STAT3 inhibition/deletion using more than one platform and additional cell lines to verify the impact of STAT3 loss on OS cell growth.

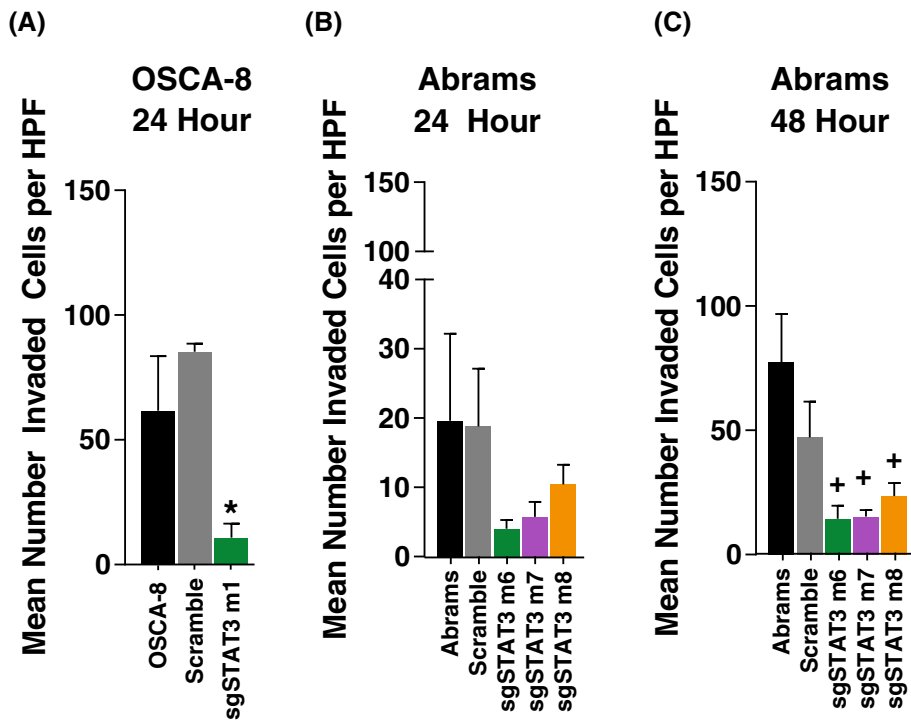


FIGURE 4 Loss of STAT3 decreases invasive capacity of canine OS cell lines. The invasive capacity of OSCA8 (A) and Abrams (B–C) cells with and without STAT3 expression is shown as the mean of three biologic replicates. $p < .05$ was considered significant. M(#)= monoclonal knockout cell line. * $p < .05$; + $p < .01$; # $p \leq .001$. Error bars represent SE. Statistical comparisons are made using the wild-type cell line as the reference.

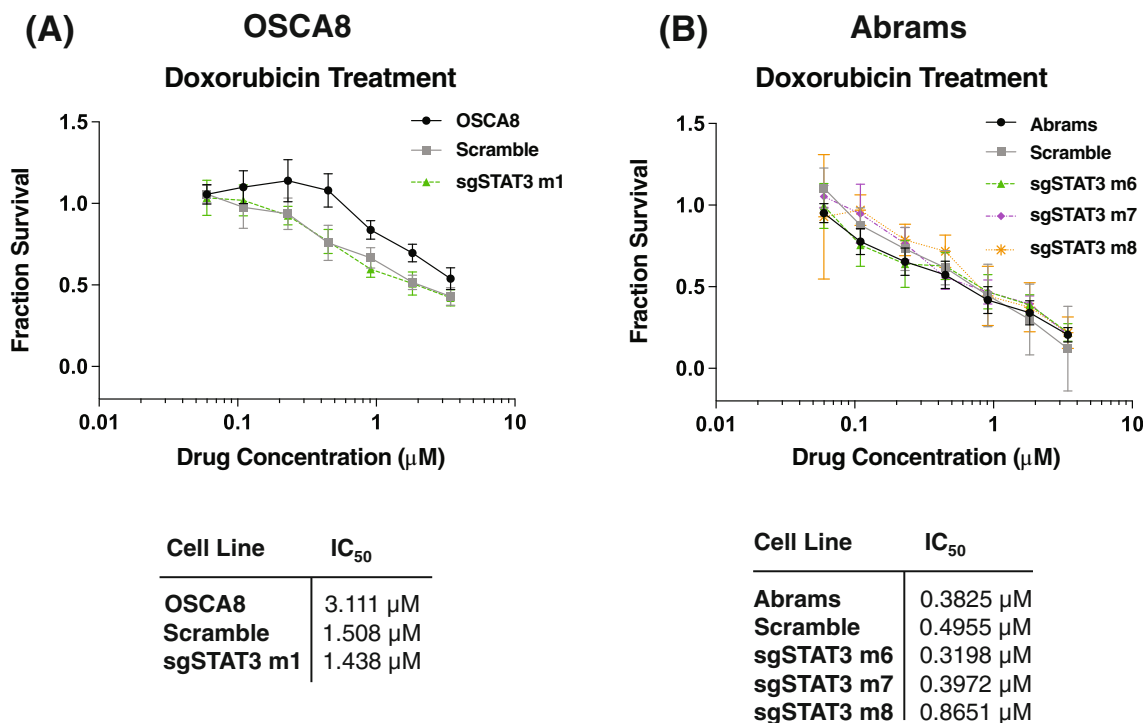


FIGURE 5 STAT3 deletion does not sensitize OS cells to doxorubicin. Proliferation in (A) OSCA8 and (B) Abrams cell lines exposed to increasing concentrations of doxorubicin are displayed as a fraction of an untreated control after exposure doxorubicin for 24 h. Error bars indicate the SD across three biologic replicates.

While typically considered in the context of its role as a nuclear transcription factor, STAT3 is thought to have a multi-faceted role in tumour metabolism, with activity increasingly attributed to transcriptional and non-transcriptional activities in the cytosol and mitochondria.^{10,13,39,40} Specifically, STAT3 has been identified in the

mitochondria associated with ETC Complexes and mitochondrial DNA, suggesting that the nuclear and metabolic features of STAT3 are coordinated to promote oncogenic phenotypes.^{13,14,41,42} Additionally, STAT3 appears to activate aerobic glycolysis and inhibit mitochondrial oxidative phosphorylation (OXPHOS) through its action as a

nuclear transcription factor.⁴²⁻⁴⁴ Our data demonstrate that loss of STAT3 modulates features of aerobic glycolysis in OS cell lines without affecting cellular proliferation. Taken together this implies that canine OS lines can maintain bioenergetic processes (ATP production) through oxidative phosphorylation when glycolysis is compromised upon STAT3 deletion, sustaining cellular proliferation.

Not surprisingly, as downregulation of aerobic glycolysis was incomplete in STAT3-deficient cells, concentrations of intracellular lactate were variable in the absence of STAT3. This likely indicates the presence of alternate mechanisms for maintenance of aerobic glycolysis in STAT3-deficient cell lines, such as modulation of glucose uptake and altered glycolytic enzyme or monocarboxylate transporter (MCT1, MCT4) activity to facilitate lactate exchange. Notably, these effects were identified *in vitro*, without considering the metabolic relationship between the tumour and stromal cells.⁴⁵ Indeed, metabolic plasticity promotes cell survival and growth in the metastatic microenvironment across several tumour types, and metabolic pathway dysregulation alters OS metastatic progression in murine models.⁴⁶⁻⁴⁹ Consequently, inhibition of STAT3 function *in vivo* may be insufficient to impact tumour cell biology without concordant blockade of additional key cellular proteins (such as MCT1/4) that support this plasticity.

In conclusion, these data further support the contribution of STAT3 to aerobic glycolysis and cellular invasive capacity in canine OS. Further interrogation is warranted to identify how best to leverage STAT3 inhibition as a therapeutic strategy in OS through rational combinatorial targeting of key pathways that influence OS metabolic plasticity and drive metastatic capacities.

ACKNOWLEDGEMENT

The content is solely the responsibility of the authors and does not necessarily represent the official views of the National Institutes of Health.

FUNDING INFORMATION

This research was funded by Sarcoma Foundation of America: C. London (PI); H. Gardner (Co-I); Morris Animal Foundation Fellowship: H. Gardner (PI); C. London (mentor); Morris Animal Foundation: C. London (PI); H. Gardner (Co-I); Animal Cancer Foundation: C. London (PI); H. Gardner (Co-I); NCI NIH Studies of Childhood Sarcoma P01CA165995: C. London (Project 2 & Core C); NIH Office of the Director, Grant/Award Number: K01OD019923: J. Fenger (PI); NCI NIH Career Development Award K08CA201638: R. Roberts (PI); NIH Office of the Director, Grant/Award Number: K01OD028268: H. Gardner (PI).

CONFLICT OF INTEREST

The authors declare no potential conflict of interest.

DATA AVAILABILITY STATEMENT

The data that supports the findings of this study are available in the supplementary material of this article.

ORCID

Heather L. Gardner  <https://orcid.org/0000-0001-6007-6144>

REFERENCES

- Kim C, Matsuyama A, Mutsaers AJ, Woods JP. Retrospective evaluation of toceranib (Palladia) treatment for canine metastatic appendicular osteosarcoma. *Can Vet J*. 2017;58(10):1059-1064.
- Laver T, London CA, Vail DM, Biller BJ, Coy J, Thamm DH. Prospective evaluation of toceranib phosphate in metastatic canine osteosarcoma. *Vet Comp Oncol*. 2018;16(1):E23-E29.
- Sakthikumar S, Elvers I, Kim J, et al. SETD2 is recurrently mutated in whole-exome sequenced canine osteosarcoma. *Cancer Res*. 2018;78(13):3421-3431.
- Gardner HL, Sivaprakasam K, Briones N, et al. Canine osteosarcoma genome sequencing identifies recurrent mutations in DMD and the histone methyltransferase gene SETD2. *Commun Biol*. 2019;2:266.
- LeBlanc AK, Mazcko CN. Improving human cancer therapy through the evaluation of pet dogs. *Nat Rev Cancer*. 2020;20(12):727-742.
- Chu S, Skidmore ZL, Kunisaki J, et al. Unraveling the chaotic genomic landscape of primary and metastatic canine appendicular osteosarcoma with current sequencing technologies and bioinformatic approaches. *PLoS One*. 2021;16(2):e0246443.
- Bid HK, Oswald D, Li C, London CA, Lin J, Houghton PJ. Anti-angiogenic activity of a small molecule STAT3 inhibitor LLL12. *PLoS One*. 2012;7(4):e35513.
- Onimoe GI, Liu A, Lin L, et al. Small molecules, LLL12 and FLLL32, inhibit STAT3 and exhibit potent growth suppressive activity in osteosarcoma cells and tumor growth in mice. *Invest New Drugs*. 2012;30(3):916-926.
- Tsuji S, Ohama T, Nakagawa T, Sato K. Efficacy of an anti-cancer strategy targeting SET in canine osteosarcoma. *J Vet Med Sci*. 2019;81(10):1424-1430.
- Huynh J, Chand A, Gough D, Ernst M. Therapeutically exploiting STAT3 activity in cancer - using tissue repair as a road map. *Nat Rev Cancer*. 2019;19(2):82-96.
- Hirano T, Ishihara K, Hibi M. Roles of STAT3 in mediating the cell growth, differentiation and survival signals relayed through the IL-6 family of cytokine receptors. *Oncogene*. 2000;19(21):2548-2556.
- Srivastava J, DiGiovanni J. Non-canonical Stat3 signaling in cancer. *Mol Carcinog*. 2016;55(12):1889-1898.
- Wegrzyn J, Potla R, Chwae YJ, et al. Function of mitochondrial Stat3 in cellular respiration. *Science*. 2009;323(5915):793-797.
- Gough DJ, Corlett A, Schlessinger K, Wegrzyn J, Larner AC, Levy DE. Mitochondrial STAT3 supports Ras-dependent oncogenic transformation. *Science*. 2009;324(5935):1713-1716.
- Zhang Q, Raje V, Yakovlev VA, et al. Mitochondrial localized Stat3 promotes breast cancer growth via phosphorylation of serine 727. *J Biol Chem*. 2013;288(43):31280-31288.
- Yu H, Lee H, Herrmann A, Buettner R, Jove R. Revisiting STAT3 signalling in cancer: new and unexpected biological functions. *Nat Rev Cancer*. 2014;14(11):736-746.
- Lee H, Zhang P, Herrmann A, et al. Acetylated STAT3 is crucial for methylation of tumor-suppressor gene promoters and inhibition by resveratrol results in demethylation. *Proc Natl Acad Sci U S A*. 2012;109(20):7765-7769.
- Fossey SL, Liao AT, McCleese JK, et al. Characterization of STAT3 activation and expression in canine and human osteosarcoma. *BMC Cancer*. 2009;9:81.
- Couto JI, Bear MD, Lin J, et al. Biologic activity of the novel small molecule STAT3 inhibitor LLL12 against canine osteosarcoma cell lines. *BMC Vet Res*. 2012;8:244.
- Fossey SL, Bear MD, Lin J, et al. The novel curcumin analog FLLL32 decreases STAT3 DNA binding activity and expression, and induces apoptosis in osteosarcoma cell lines. *BMC Cancer*. 2011;11:112.
- Fossey SL, Bear MD, Kisseberth WC, Pennell M, London CA. Oncostatin M promotes STAT3 activation, VEGF production, and invasion in osteosarcoma cell lines. *BMC Cancer*. 2011;11:125.

22. Bid HK, Roberts RD, Cam M, et al. Δ Np63 promotes pediatric neuroblastoma and osteosarcoma by regulating tumor angiogenesis. *Cancer Res.* 2014;74(1):320-329.
23. Cam M, Gardner HL, Roberts RD, et al. Δ Np63 mediates cellular survival and metastasis in canine osteosarcoma. *Oncotarget.* 2016;7(30):48533-48546.
24. Gross AC, Cam H, Phelps DA, et al. IL-6 and CXCL8 mediate osteosarcoma-lung interactions critical to metastasis. *JCI Insight.* 2018;3(16). doi:10.1172/jci.insight.99791
25. Porporato PE, Payen VL, Pérez-Escuredo J, et al. A mitochondrial switch promotes tumor metastasis. *Cell Rep.* 2014;8(3):754-766.
26. Das S, Idate R, Cronise KE, Gustafson DL, Duval DL. Identifying candidate druggable targets in canine cancer cell lines using whole-exome sequencing. *Mol Cancer Ther.* 2019;18(8):1460-1471.
27. O'Donoghue LE, Rivest JP, Duval DL. Polymerase chain reaction-based species verification and microsatellite analysis for canine cell line validation. *J Vet Diagn Invest.* 2011;23(4):780-785.
28. Gardner HL, Ripsey SB, Bear MD, et al. Phase I/II evaluation of RV1001, a novel PI3Kdelta inhibitor, in spontaneous canine lymphoma. *PLoS One.* 2018;13(4):e0195357.
29. Sanjana NE, Shalem O, Zhang F. Improved vectors and genome-wide libraries for CRISPR screening. *Nat Methods.* 2014;11(8):783-784.
30. Benjamin D, Robay D, Hindupur SK, et al. Dual inhibition of the lactate transporters MCT1 and MCT4 is synthetic lethal with metformin due to NAD⁺ depletion in cancer cells. *Cell Rep.* 2018;25(11):3047-3058 e4.
31. Orellana EA, Kasinski AL. Sulforhodamine B (SRB) assay in cell culture to investigate cell proliferation. *Bio Protoc.* 2016;6(21). doi:10.21769/BioProtoc.1984
32. Liao AT, McCleese J, Kamerling S, Christensen J, London CA. A novel small molecule Met inhibitor, PF2362376, exhibits biological activity against osteosarcoma. *Vet Comp Oncol.* 2007;5(3):177-196.
33. Gilliam LAA, Fisher-Wellman KH, Lin CT, Maples JM, Cathey BL, Neuffer PD. The anticancer agent doxorubicin disrupts mitochondrial energy metabolism and redox balance in skeletal muscle. *Free Radic Biol Med.* 2013;65:988-996.
34. Szczepanek K, Lesnfsky EJ, Larner AC. Multi-tasking: nuclear transcription factors with novel roles in the mitochondria. *Trends Cell Biol.* 2012;22(8):429-437.
35. Yu PY, Gardner HL, Roberts R, et al. Target specificity, in vivo pharmacokinetics, and efficacy of the putative STAT3 inhibitor LY5 in osteosarcoma, Ewing's sarcoma, and rhabdomyosarcoma. *PLoS One.* 2017;12(7):e0181885.
36. Yang L, Lin S, Xu L, Lin J, Zhao C, Huang X. Novel activators and small-molecule inhibitors of STAT3 in cancer. *Cytokine Growth Factor Rev.* 2019;49:10-22.
37. Hariharan S, Phelps DA, Houghton PJ. Abstract 1128: role of STAT3 in pediatric sarcoma cell lines. *Cancer Res.* 2016;76(14_Supplement):1128.
38. Rokavec M, Öner MG, Li H, et al. IL-6R/STAT3/miR-34a feedback loop promotes EMT-mediated colorectal cancer invasion and metastasis. *J Clin Invest.* 2014;124(4):1853-1867.
39. Garama DJ, White CL, Balic JJ, Gough DJ. Mitochondrial STAT3: powering up a potent factor. *Cytokine.* 2016;87:20-25.
40. Gough DJ, Koetz L, Levy DE. The MEK-ERK pathway is necessary for serine phosphorylation of mitochondrial STAT3 and Ras-mediated transformation. *PLoS One.* 2013;8(11):e83395.
41. Liu B, Palmfeldt J, Lin L, et al. STAT3 associates with vacuolar H⁺-ATPase and regulates cytosolic and lysosomal pH. *Cell Res.* 2018;28(10):996-1012.
42. Avalle L, Camporeale A, Morciano G, et al. STAT3 localizes to the ER, acting as a gatekeeper for ER-mitochondrion Ca²⁺ fluxes and apoptotic responses. *Cell Death Differ.* 2019;26(5):932-942.
43. Li M, Jin R, Wang W, et al. STAT3 regulates glycolysis via targeting hexokinase 2 in hepatocellular carcinoma cells. *Oncotarget.* 2017;8(15):24777-24784.
44. Lee M, Hirpara JL, Eu JQ, et al. Targeting STAT3 and oxidative phosphorylation in oncogene-addicted tumors. *Redox Biol.* 2019;25:101073.
45. Sanita P, Capulli M, Teti A, et al. Tumor-stroma metabolic relationship based on lactate shuttle can sustain prostate cancer progression. *BMC Cancer.* 2014;14:154.
46. Ren L, Hong ES, Mendoza A, et al. Metabolomics uncovers a link between inositol metabolism and osteosarcoma metastasis. *Oncotarget.* 2017;8(24):38541-38553.
47. Labuschagne CF, Cheung EC, Blagih J, Domart MC, Vousden KH. Cell clustering promotes a metabolic switch that supports metastatic colonization. *Cell Metab.* 2019;30(4):720-734 e5.
48. Tseng CW, Kuo WH, Chan SH, Chan HL, Chang KJ, Wang LH. Transketolase regulates the metabolic switch to control breast cancer cell metastasis via the alpha-ketoglutarate signaling pathway. *Cancer Res.* 2018;78(11):2799-2812.
49. Vasseur S, Tomasini R, Tournaire R, Iovanna JL. Hypoxia induced tumor metabolic switch contributes to pancreatic cancer aggressiveness. *Cancers.* 2010;2(4):2138-2152.

SUPPORTING INFORMATION

Additional supporting information may be found in the online version of the article at the publisher's website.

How to cite this article: Gardner HL, Fenger JM, Roberts RD, London CA. Characterizing the metabolic role of STAT3 in canine osteosarcoma. *Vet Comp Oncol.* 2022;20(4):817-824. doi:10.1111/vco.12841